Available online at: www. Ijcoe.org

Experimental study of gas flow regime criteria in underwater gas-saturated liquid blowouts

Maryam Bafandeh[1], Abbas-Ali Ali Akbari Bidokhti[2], Mojtaba Ezam[3], Majid Ghodsi Hasanabad[4], Sara Allahyari Beyk[5]

[1]*Department of Physical Oceanography, Tehran Science and Research Branch, Islamic Azad University, Tehran, Iran, maryam.bafandeh88@gmail.com*
[2]*Professor, Institute of Geophysics, University of Tehran, Tehran, Iran, bidokhti@ut.ac.ir*
[3]*Associate Professor, Department of Physical Oceanography, Tehran Science and Research Branch, Islamic Azad University, Tehran, Iran, ezam@srbiau.ac.ir*
[4]*Associate Professor, Department of Mechanical Engineering, Tehran Science and Research Branch, Islamic Azad University, Tehran, 1477893855, Iran*
[5]*Department of Physical Oceanography, Tehran Science and Research Branch, Islamic Azad University, Tehran, Iran, s.allahyaribeik@gmail.com*

ARTICLE INFO

Article History:
Received 12 Jan 2026
Accepted 8 June 2026
Available online ….

Keywords:
Bubbly Jet
Multiphase Flow
Underwater Blowout
Oil and Gas blowout
Underwater Waste Disposal

ABSTRACT

In a series of laboratory experiments, CO_2-saturated freshwater at different volumetric gas to liquid ratios (GLR) and different flow momentums was injected at the bottom of square cross-section open-top basins filled with homogeneous saltwater as well as stratified saltwater. Flow visualization of the experiments and comparison of different criteria for discerning the gas flow regimes showed that Wallis (1969) critical velocity criterion and Payne and Prince (1975) modified Froude number criterion are more suitable to distinguish the gas flow regimes in gas-saturated liquid blowouts. The other evaluated criteria of modified Froude number, Reynolds number, and modified Weber number, overestimate the ratio of inertia and bubble destructive forces to breakup resisting forces in gas-saturated liquid blowouts. It seems that off-source rapid formation of a huge number concentration of minute bubbles in the zone of flow establishment and momentum-driven region decreases the inertia and bubble destructive forces in gas-saturated liquid blowouts when compared to bubbly jets of similar GLR and flow rates.

1- INTRODUCTION

Discerning the gas flow regime in liquid basins has significant implications in the industry. Jet instabilities and dispersed phase break-up processes have been widely studied in different aspects of science and applications, including (but not limited to) water treatment, metallurgy, chemical engineering, and environmental engineering (Oguz & Prosperetti, 1993). In liquid-gas systems, fluid dynamics of the dispersed phase, the liquid-gas force coupling, and the mass transfer rate depend on the bubble size and the amount of contact surface between two immiscible fluids; as such, the core of numerical models simulating such processes is the flow regime and breakup processes of the dispersed phase in the basin (Sun, Cao, Liang, & Bian, 2020).

One of the implications areas of jet instability studies is in marine applications such as CO_2 sequestration in oceans as well as marine accidental underwater oil and gas blowouts. Generally, in live-oil underwater blowouts from offshore facilities, some amount of gas partitions from the live oil. Meanwhile, stratification in the water column may cause the pollutant plume to peel and trap at finite heights. In stratified plumes, the volumetric ratio of gas phase to liquid phase (GLR) and the slip velocity of bubbles, which in turn is a function of bubble size, can significantly affect the dynamics of the pollutant plume.

Zhao et al. (2016) used the numerical model VDROP-J (L. Zhao et al., 2014) to simulate the processes of gas separation, bubble formation, dissolution, expansion, and fate of bubbles in underwater oil blowouts. They showed that minute bubbles would dissolve in seawater bulk while the bubbles that are bigger than a certain estimable size would reach the sea surface. Encountering different physical-chemical processes they argued that bubble size is the key factor in determining the bubbles fate, whether they reach the surface, dissolve in liquid phase or form hydrates.

Fate of bubbles in gas-liquid plumes directly affects plume peeling and trapping heights and consequently plays a crucial role in plume surfacing time, surfacing location and the pollutant distribution on sea surface. As such determining the gas phase break-up processes in accidental underwater oil and gas blowouts is important for predicting the environmental impact of the accident, risk assessment and response planning.

Contrary to deepwater blowouts where the contaminant plume most likely would trap below sea surface (Johansen, Brandvik, & Farooq, 2013) the effect of bubble size on increasing the plume peeling and trapping heights is more significant in moderate and shallow waters. As such a proper estimation of gas phase flow regime and bubble size distribution is crucial for realistic oil and gas plume fate prediction and estimating the extent of contaminant distribution on the sea surface.

Different criterions for the prediction of gas flow regimes (jetting, transitional, or bubbling) in gas-saturated liquid blowouts in stagnant waters are evaluated in this research, using a series of laboratory experiments. Based on the findings of this research, it is possible to predict the gas flow regimes in underwater live oil blowouts and conduct a pre-assessment. Knowledge about the qualitative behavior of the pollutant plume and quantitative estimation of oil and gas surfacing time, surfacing distance from the blowout point, and the extent of pollutant distribution on the sea surface are important for safety-related and environmentally-related applications.

The innovative approach of the present study lies within the experimental method where gas-saturated liquid is released in the basin to qualitatively investigate the effect of off-source bubble formation on gas flow regime during gas-saturated liquid blowouts (Brandvik et al., 2015) the majority of previous experimental studies were conducted by simultaneous gas pumping and liquid pumping aiming to inject the gas in liquid pipeline downstream to release point for mixing the gas flow with the liquid flow.

1-1 The effect of Bubble sie distribution on plume dynamics

Flow properties, geometry of the blowout opening, seawater density, viscosity, and surface tension are some of the major variables that cause a certain plume GLR to produce different sizes of gas bubbles. The effect of changes in these criterions on dynamic parameters of single-phase gas plumes and two-phase gas-liquid plumes in liquid basins has been the subject of several experimental and numerical research (Bafandeh, Bidokhti, Lari, & Ezam, 2022; Brandvik et al., 2015; Socolofsky & Adams, 2005; Sun et al., 2020; L. Zhao et al., 2017; L. Zhao et al., 2014).

In stratified two-phase gas-liquid plumes, gas bubbles separate from the entrained seawater plume and tend to lift the liquid phase further upward in the water column than the level of neutral buoyancy (trapping height). That is due to the imparted energy from gas bubbles to the liquid phase as a function of bubble slip velocity. Thereafter, the plume will continue to rise above the trapping height until it reaches a peeling height, where dispersed phase buoyancy can no longer lift the entrained seawater (Socolofsky, Adams, & Sherwood, 2011).

In two-phase gas-liquid blowouts, the size of bubbles directly affects the slip velocity of the bubbles relative to the rest of the plume fluids. Momentum exchange between gas phase and liquid phase per unit volume Φ is the opposite of the sum of the momentum transfer rate of forces exerted by liquid on bubbles present in unit volume (Eq. 1). The exerted forces can be listed as drag force, D, lift force, L, virtual mass force, VM, Basset history, H, and the gravity and far-field pressure contributions, $F_G + F_P$ (Delnoij, Kuipers, & van Swaaij, 1997).

$$\Phi V_{cell} = \sum_i (F_{Di} + F_{VMi} + F_{Li} + F_{Hi} + F_G + F_P) \quad (1)$$

The forces acting from bubbles to the liquid are attributed to bubble size, either directly or through the bubble slip velocity (U_{si}), which in turn is also related to the size of bubbles (Delnoij et al., 1997).

Lift force and Basset history force are of several orders of magnitude smaller than drag force and other applied forces in Eq.1 and can be neglected in calculations of bubbly plumes dynamics (Delnoij et al., 1997; L. Zhao et al., 2017). Accordingly, Zhao et al. (2017) formulated the impact of bubbles on the mixing energy of the jet/plume systems (Eqs. 2 and 3).

$$\varepsilon_i = \frac{F_{imposed} U_{si} N_i}{\rho_c} \quad (2)$$

$$F_{imposed} = \frac{1}{2} C_D A_b \rho_C |U_b - U_c| (U_b - U_c) + \frac{1}{2} m_c \left(\frac{dU_b}{dt} - \frac{dU_c}{dt}\right) \quad (3)$$

Here N_i $(number\ of\ bubbles/m^3)$ is the number concentration of bubbles with a specific size d_i in the volume of water in concern. ε_i is the energy dissipation rate generated from the rise of this group of bubbles, C_D is the drag coefficient, and A_b is the projected area of the bubble (m^2). U_b and U_c are the velocity of bubbles and continues phase respectively (m/s), m_c is the added mass of the liquid which in the absence of bubbles is accelerated and ρ_c is the density of the continues phase.

One of the major influential factors on number concentration of bubbles and size of bubbles in gas-saturated liquid blowouts is the gas flow regime of the blowout. Bubbling gas flow regime may produce large bubbles with lower number concentration of bubbles while jetting regime develops small bubbles with higher number concentration of bubbles.

1-2 Gas flow regime criterions in Gas-saturated liquid blowouts in stagnant water

Blowout flow specifications and ambient conditions (pressure, temperature, cross flows, etc.) have major effects on the bubbling regime of plumes, while the shape, surface roughness, and size of the opening also play significant roles in bubble size and number concentration of bubbles (Goda, Iguchi, Sasaki, & Kiuchi, 2005; Kubasch, 2001; Tsuge, Tezuka, & Mitsudani, 2006).

Irrgang et al (2012) classified the gas flow regimes in liquid basins into three main categories of static bubbling, dynamic bubbling, and jetting regimes. They studied Payne and Prince (1975) and Hoefele and Brimacombe (1978) correlations of gas flow regime transition in liquid basins as two of the most commonly accepted correlations. They argued that in the static bubbling regime, the equality between surface tension and bubble buoyancy forces plays a significant role in the bubble formation process and also stated that bubble volume is governed by the orifice diameter and surface roughness, independent from the gas flow rate.

Oguz and Prosperetti (1993) introduced a critical value for gas flow rate (Q_{cr}) above which the gas bubble radius at detachment is proportional to $Q^{2/5}$ where Q is the gas flow rate, D_0 is the nozzle internal diameter, σ is the liquid surface tension, ρ is the liquid density, and g is the gravitational acceleration (Eq.4).

$$Q_{cr} = \pi \left(\frac{16}{3g^2}\right)^{\frac{1}{6}} \left(\frac{\sigma D_0}{\rho}\right)^{\frac{5}{6}} \quad (4)$$

In Oguz and Prosperetti (1993) correlation, for $Q < Q_{cr}$ the bubble radius can be as small as Fritz radius R_F (Eq. 5) where the buoyancy and surface tension forces are in balance. Oguz and Prosperetti (1993) argued that for static bubbling regime, R_F is the smallest possible bubble radius in quiescent water detached from a nozzle with a given internal diameter of D_0.

In a dynamic bubbling regime, both bubble volume and frequency of bubble formation increase with increasing the gas flow rate. For $Q > Q_{cr}$ Oguz and Prosperreti correlation for radius of the bubbles is proportional to gas flow rate (Eq.6),

$$R_F = \left(\frac{3}{2}\frac{\sigma D_0}{\rho g}\right)^{\frac{1}{3}} \quad (5)$$

$$\bar{R} = \left(\frac{9}{8\pi^2}\frac{Q^2}{g}\right)^{\frac{1}{5}} \quad (6)$$

Payne and Prince (1975) correlation (Eqs. 7 and 8) is based on the relation between the modified Froude number Fr^* and the ratio of basin liquid height H to the orifice diameter D_o, above which jetting regime will occur.

$$\frac{H}{D_o} = 1.5Fr^* \tag{7}$$

$$Fr^* = U_0\sqrt{\rho_g/(D_o g(\rho_l - \rho_g))} \tag{8}$$

Hoefele (1978) criterion is based on the correlation between Mach number $M' = U_0/C$ and density ratio of liquid and gas phases above which jetting regime occurs (Eq.9). Here C is the speed of sound in air

$$M'\left(\frac{\rho_g}{\rho_l}\right)^{0.5} = 0.009 \tag{9}$$

Bubbling process in gas-saturated liquid blowouts starts at pressure drop points and the amount of released gas is relative to the gas solubility in liquid at initial pressure and decreased pressure (Gros, Reddy, Nelson, Socolofsky, & Arey, 2016). In underwater blowouts, pressure drop may happen during pipeline transfer (due to pipe internal friction, change of cross section area, fittings, etc) and across the plume source nozzle (due to orifice effect). Additionally, since neither water nor bubbles are clean even in laboratory (L. Zhao et al., 2017) another form of gas separation commences after the release in ambient water (off-source bubble formation). This form can be considered similar to formation of bubbles with phase change which involves an initial state of a gas dissolved in liquid and later stage of bubble formation (nucleation), similar to boiling or cavitation processes (Clift, Grace, & Weber, 2005). The radius of bubbles formed in bubble nucleation can be estimated by surface tension of ambient fluid and the internal pressure of bubbles at local pressure (Eq.10). In off-source bubble formation, internal pressure of bubbles compensates the surface tension (σ) of the ambient liquid (Clift et al., 2005).

$$d_{eq} = 4\sigma/(P_v + P_g - P_l) \tag{10}$$

Here d_{eq} is the bubble's equivalent diameter, P_g is the partial pressure of non-condensable gas, P_v is the vapor pressure of the liquid at a given temperature, and P_l is the local pressure.

Off-source bubble formation is a time, pressure, and temperature dependent process and happens after the release of gas-saturated fluid from the nozzle (Gros et al., 2016) at the bubbly jet region ($z > 0.1l_M$) and bubbly plume region ($z > 5l_M$).

Here $l_M = M_0^{0.75}/F_0^{0.5}$ is the characteristic plume length, z represents the axial distance from the plume source, and M_0 and F_0 are the kinematic momentum and buoyancy flux of the blowout at the source, respectively (Lima Neto, 2012) Contrary to off-source bubble formation, pressure drop through the pipeline and bubble formation due to pressure drop across the plume source nozzle will cause the plume flow to become effervescent at the blowout nozzle. Based on flow and ambient parameters, there can be three different flow regimes of bubbling (static), transitional (dynamic bubbling), or jetting (atomization) release. Wallis (1969), Payne and Prince (1975), Hoefele and Brimacombe (1979) and Zhao and Iron (1990) criterions are each cited in different occasions by different researchers as the correlations commonly accepted for discerning the gas flow regime in underwater blowouts (Bie, Ye, & Hao, 2016; Cai, Shen, Shen, & Dai, 2010; Irrgang, Hinrichsen, & Lau, 2012; Kubasch, 2001; Miao et al., 2018). While each of the criterions are applicable in certain flow and ambient conditions, there might be cases that none of the criterions can define changes of flow patterns from bubbling to jetting regime (Kubasch, 2001).

Wallis (1969) has pointed on a critical gas flow velocity from the nozzle tip ($U_{0critical}$) above which jetting regime occurs (Eq.11).

$$U_{0critical} = 1.25\left[\frac{4\sigma}{g(\rho_{liq}-\rho_{gas})D_0^2}\right]^{0.5}\left[\frac{g\sigma(\rho_{liq}-\rho_{gas})}{\rho_{gas}^2}\right]^{0.25} \tag{11}$$

Here σ is the surface tension of the ambient liquid and D_o is the nozzle tip diameter.

When the flow velocity at the plume source nozzle is low, the interface of the gas phase with ambient water is smooth, and the flow falls in a bubbling regime. Zhao and Iron (1990) showed that when the flow Weber number exceeds the critical Weber number ($We_{critical}$), the bubbles' surface starts to ripple and bubbles start to break into small gas particles. Small gas particles are then pushed into the liquid phase, while the liquid is also pushed into the gas phase. The small droplets pushed into the gas phase are easily accelerated, and thus the gas momentum is transferred to the liquid droplets. This momentum can elongate the bubble and disrupt the interface of gas bubbles with liquid even further. The mixture of gas and liquid droplets can then push deeply into the liquid. Therefore, discrete bubble release transforms to continuous gas flow and consequently the flow falls into the jetting regime. The critical Weber number above which the jetting regime starts is given in Eq.12 (Y.-F. Zhao & Irons, 1990):

$$We_{critical} = \frac{\rho_{gas}\, U_0^2\, D_0}{\sigma} \geq 10.5\sqrt{\frac{\rho_{liq}}{\rho_{gas}}} \qquad (12)$$

Martinez-Bazan et al. (1999) suggest that high values of Ohnesorge number ($Oh = \mu/(\rho\sigma D)^{1/2}$) and Reynolds number ($Re = \rho UD/\mu$) are required for jetting (atomization) regime. Johanson et al (2013) plotted the result of Neto et al. (2008) experiments of bubbly water jets on Ohnesorge vs. Reynolds number diagram and found that it is promising that the transition lines of constant Weber number derived from single liquid flows, also applies to bubbly jets and the mean bubble size. Johansen et al. (2013), after Tang and Masutani (2003) used boundaries of constant Weber numbers $We = c^2$ between laminar and transitional breakup regimes ($c = 5.5$) and between transitional and turbulent (atomization) breakup regimes ($c = 18$) in liquid-liquid jet blowouts ($We = \rho_{jet\,fluid}\, U_0^2\, D_0/\sigma$). Here, c is a constant of proportionality.

Hoeffel and Brimacombe (1979) used the correlation of Mach number with gas to liquid density ratio (Eq.9) and developed a bubble-jet behavior diagram based on the gas to liquid density ratio and the modified Froude number. Using the density ratio of the gas phase to the liquid phase on the diagram and delineating the modified Froude number of a gas flow in a liquid basin, one can easily find out whether the flow falls in the bubbling, transitional or jetting regime. The modified Froude number as used in Hoefele and Brimacombe (1979) criterion is given in Eq.13.

$$F_{rm} = \frac{\rho_{gas} U_0^2}{g(\rho_{liq} - \rho_{gas}) D_0} \qquad (13)$$

Krishnapisharodi and Iron (2013) suggested that the modified Froude number, as a function of gas flow rate (Eq.14), would also be a comprehensive characteristic for underwater gas jets.

$$F_{rm} = \frac{\rho_{gas} Q^2}{g(\rho_{liq} - \rho_{gas}) D_0^5} \qquad (14)$$

They also argued that the modified Froude number is not an appropriate characteristic for use in buoyancy driven plumes where the injected momentum is dissipated within a very short distance from the nozzle (Krishnapisharody & Irons, 2013).

The above criterions have been widely used in several industrial applications and research. Most of the previous researches were conducted based on single-phase gas flow injection at the bottom of the liquid basin, or as mentioned earlier in the present report, two-phase experiments were based on producing bubbly jets by combining gas pumping with liquid pumping within the pipeline. In the experiments of the present research, first of all, the liquid was saturated with different pre-defined gas concentration ratios, and then the gas-saturated liquids were injected at different flow rates at the bottom of the liquid basin. Laboratory experiments were visually analyzed for qualitative evaluation of gas flow regime criterions in gas-saturated liquid blowouts.

2- MATERIAL AND METHODS

A series of laboratory tests was conducted in a transparent plexiglass square cross-section open-top basin of 1.20×0.45×0.45 m dimensions, which was filled with homogenous or stratified saltwater up to the level of 1.05 m height (height to width aspect ratio = 2.33).

Plume flow was produced by a 12-liter pressurized vessel filled with tap water ($\rho = 998.5\ kg/m^3$ at $T = 20$ ℃), colored by foodgrade colors and pressurized with CO_2 gas (99% purity). The laboratory experiment setup is schematically shown in Fig. 1.

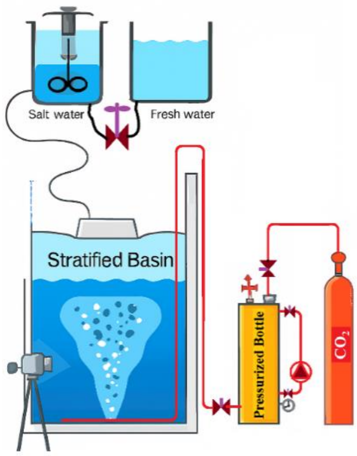

Fig.1 Schematic diagram of the setup for laboratory experiments.

After saturation of water with CO_2 at a pressure of $5\,kg/cm^2$ in the pressurized vessel, the pressure of the vessel was decreased to $1\,kg/cm^2$, $2\,kg/cm^2$ and $3\,kg/cm^2$ for different test groups of 1bar, 2bar, and 3bar, respectively. The pressure of the vessel was maintained constant at the desired pressures with an adjustable pressure relief and an adjustable pressure regulating valve.

The constant vessel's internal pressures were used to pump out the colored and CO_2-saturated water through a series of hoses and copper tubes to the bottom of the stratified basin, where a circular hole of 3.5 mm in diameter was prepared in a vertical upward direction. The photo of experimental setup in the laboratory is shown in Fig 2.

Fig.2 Experimental setup for gas flow visualization in the laboratory.

3- Results and

A total number of 30 experimental tests were conducted. The experiments were recorded with ~10 frames per second photography (596 fpm), and images were analyzed visually on a mesh grid of 2.5 mm resolution. Bubbles diameter in laboratory experiments was roughly measured using a 2.5 mm mesh grid, as a precise bubble diameter was not required to investigate the gas flow regimes. The list of different groups of experiments is given in Table 1, and samples of flow visualizations of gas-saturated liquid blowouts in stratified basins are shown in Fig. 3. The bubble formation in the test setup is shown in Fig. 4.

Table 1. list of laboratory experiments

Test Group	Test No.	Flow rate (m^3/s)	CO_2 saturation pressure (Kg/cm^2)	Density of the plume fluid (Kg/m^3)	Reynolds number	Plume GLR at nozzle tip	Temperature (°C)	Basin's bottom layer salinity (ppt)	Buoyancy frequency of the basin (s^{-1})
1bar	T-5	0.0000429	1	1001	15603	0.131	15.4	15	0.283
1bar	T-6	0.0000429	1	1001	15603	0.131	18	25	0.323

1bar	T-7	0.0000429	1	1001	15603	0.131	12.8	36	0.395
1bar	T-8	0.0000429	1	1001	15603	0.131	21	45	0.437
1bar	T-9	0.0000429	1	1001	15603	0.131	16.7	45	0.441
1bar	T-10	0.0000429	1	1001	15603	0.131	18	55	0.460
1bar	T-12	0.0000429	1	1001	15603	0.131	20	35	0
1bar	T-13	0.0000429	1	1001	15603	0.131	20	35	0
2bar	T-17	0.0000645	2	1001	23459	0.235	14	35	0
2bar	T-18	0.0000645	2	1001	23459	0.235	14	35	0
2bar	T-19	0.0000645	2	1001	23459	0.235	20	35	0
2bar	T-20	0.0000645	2	1001	23459	0.235	15.6	25	0.332
2bar	T-21	0.0000645	2	1001	23459	0.235	12	36	0.438
2bar	T-23	0.0000645	2	1001	23459	0.235	18.2	45	0.433
3bar	T-26	0.0000811	3	1001	29498	0.335	12	35	0
3bar	T-27	0.0000811	3	1001	29498	0.335	12	35	0
3bar	T-30	0.0000811	3	1001	29498	0.335	13	36	0.431

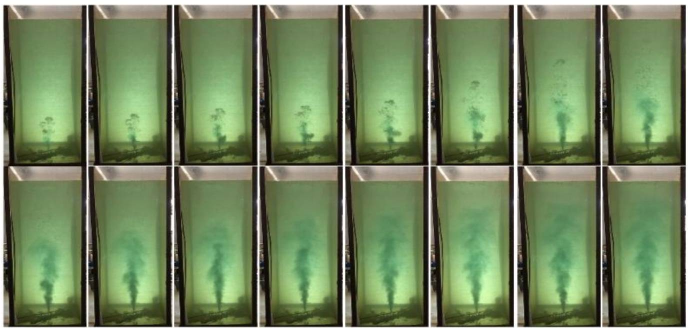

Fig.3 Sample flow visualization of gas-saturated in stratified basin

Flow visualization of 1bar test group experiments clearly depicts the presence of small bubbles of order of $10^{-4}m$ or less in diameter, along with large bubbles of order of $10^{-3}m$ in diameter within the plume. Large bubbles were continually generated from effervescent flow due to gas separation from liquid through the pipeline and across the nozzle.

These bubbles were ascending and separating from the liquid plume during the whole test duration. However, only in the initial frames of 2bar and 3bar test groups some large bubbles of order of $10^{-3}m$ in diameter were seen.

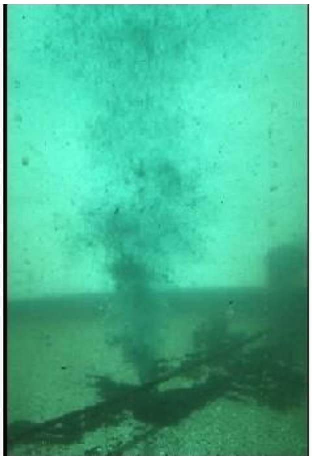

Fig.4 Bubble formation from effervescent flow in stratified water column

In 2bar and 3bar test groups, the large bubbles that were ascending to the surface disappeared after a few seconds (5 to 6 seconds), and the rest of the bubbles generated in these test groups were of order of $10^{-4}m$ or less in diameter, as the experiments were continued. The initial large bubbles of 2bar and 3bar test groups can be considered as the result of some amount of air that might had been trapped in the pipeline prior the initiation of each experiment. Presence of these few bubbles for a short duration of time can be eliminated from the experimental results. Flow visualization of the experiments and presence of almost irregular sizes of bubbles in 1bar test group suggest that this test group falls in dynamic (transitional) gas flow regime while 2bar and 3bar test groups with relatively uniform minute bubbles fall in jetting (atomizing) regime (Lima Neto, 2012).

For the case of two phase gas-liquid blowouts, Johansen et al. (2013) findings imply that a situation with a gas volume fraction (n) and a liquid volume flow (Q_L) might be represented by a liquid only experiment with an adjusted equivalent liquid volume flow $Q_E = Q_L/(1-n)^{1/2}$ and equivalent liquid only velocity $U_E = U_L/(1-n)^{1/2}$. Here gas volume fraction (n) is defined as the ratio of the gas flow rate (Q_G) to the total gas–liquid mixture flow rate at the nozzle, $n = Q_G/(Q_L + Q_G)$, and U_L is the liquid only velocity. In gas-saturated liquid blowouts of present experiments, the amount of the gas released through the pipeline and across the plume source nozzle was originally dissolved in the liquid. Assuming that in an effervescent liquid flow, the contribution of the gas phase to the momentum flux (due to the much smaller density of the gas) is negligible (Brandvik et al. 2014) we can consider the gas volume fraction (n) equal to the plume GLR at nozzle tip (Table 1).

Zhao et al. (2017) developed an expression based on the work of Johansen et al. (2013), for the equivalent liquid only exit velocity $U_{E,LO}$ and equivalent liquid only exit flow rate $Q_{E,LO}$ (Eq.15 and 16)

$$U_{E,LO} = (U_L + U_G)(1 - n\left(1 - \frac{\rho_G}{\rho_L}\right))^{1/2} \quad (15)$$

$$Q_{E,LO} = (Q_L + Q_G)(1 - n\left(1 - \frac{\rho_G}{\rho_L}\right))^{1/2} \quad (16)$$

Where U_L and U_G are the velocity of liquid phase and gas phase in the mixture respectively (m/s), $U_L = \frac{Q_L}{A_{Exit}}$, $U_G = \frac{Q_G}{A_{Exit}}$, Q_L and Q_G are the liquid and gas flow rates (m^3/s) respectively, ρ_L and ρ_G are the liquid and gas densities (kg/m^3) respectively and A_{Exit} is the cross section area of exit nozzle. Using Eqs. 15 and 16 the equivalent liquid only velocity of 1bar, 2bar and 3bar test groups are 4.701 (m/s), 7.243 (m/s) and 9.181 (m/s) respectively and the equivalent liquid only flow rates are 0.00004523 (m^3/s), 0.00006969 (m^3/s) and 0.00008833 (m^3/s) respectively.

To compare the application of mostly accepted flow regime criterions for discerning the flow regimes in gas-saturated liquid blowouts of present experiments, the criterions were applied to flow specifications of present laboratory experiments. The results of the flow regime criterions on underwater gas-saturated liquid blowouts of present research are summarized in Table 2. Table 2 shows the outputs of the correlations when equivalent liquid only flow specifications are considered as the dispersed phase characteristics in the correlations (eg. velocity, flow rate, density, etc.).

Table 2. Gas flow regime criterions in experimental results using equivalent liquid only velocities and flow rates.

salinity ppt	Characteristic	Criterion	Lower limit for Jetting regime	1bar test group	2bar test group	3bar test group
25	Critical Velocity	Wallis Critical Velocity criterion	7.121	4.701	7.243	9.181
25	Mach number	Hoefele and Brimacombe nominal Mach number criterion	0.00907	0.0137	0.0211	0.0267
25	Weber number	Zhao and Iron critical Weber number criterion	238.025	1063.91	2525.17	4056.50
25	Weber number	Tang and Masutani modified Weber number criterion	324	1063.91	2525.17	4056.50
25	Modified Froude number	Hoefele and Brimacombe velocity based modified Froude number criterion	185	39061	92711	148934
25	Modified Froude number	Hoefele and Brimacombe flow rate based modified Froude number criterion	185	390.7	927.3	1489.7
25	Modified Froude number	Payne and Prince modified Froude number criterion	200	197.6	304.4	385.9
35	Critical Velocity	Wallis Critical Velocity criterion	7.159	4.701	7.243	9.181
35	Mach number	Hoefele and Brimacombe nominal Mach number criterion	0.00910	0.0137	0.0211	0.0267
35	Weber number	Zhao and Iron critical Weber number criterion	238.78	1054.10	2501.90	4019.12
35	Weber number	Tang and Masutani modified Weber number criterion	324	1054.10	2501.90	4019.12
35	Modified Froude number	Hoefele and Brimacombe velocity based modified Froude number criterion	185	28022	66510	106844
35	Modified Froude number	Hoefele and Brimacombe flow rate based modified Froude number criterion	185	388.2	921.5	1480.3

35	Modified Froude number	Payne and Prince modified Froude number criterion	200	167.3	257.8	326.87
45	Critical Velocity	Wallis Critical Velocity criterion	7.376	4.701	7.243	9.181
45	Mach number	Hoefele and Brimacombe nominal Mach number criterion	0.00913	0.0137	0.0211	0.0267
45	Weber number	Zhao and Iron critical Weber number criterion	239.71	1010.22	2397.74	3851.79
45	Weber number	Tang and Masutani modified Weber number criterion	324	1010.22	2397.74	3851.79
45	Modified Froude number	Hoefele and Brimacombe velocity based modified Froude number criterion	185	20790	49346	79271
45	Modified Froude number	Hoefele and Brimacombe flow rate based modified Froude number criterion	185	385.9	916.1	1471.6
45	Modified Froude number	Payne and Prince modified Froude number criterion	200	144.1	222.1	281.5
55	Critical Velocity	Wallis Critical Velocity criterion	7.458	4.701	7.243	9.181
55	Mach number	Hoefele and Brimacombe nominal Mach number criterion	0.00917	0.0137	0.0211	0.0267
55	Weber number	Zhao and Iron critical Weber number criterion	240.64	992.98	2356.82	3786.07
55	Weber number	Tang and Masutani modified Weber number criterion	324	992.98	2356.82	3786.07
55	Froude number	Hoefele and Brimacombe velocity based modified Froude number criterion	185	16525	39224	63010
55	Froude number	Hoefele and Brimacombe flow rate based modified Froude number criterion	185	383.0	909.05	1460.3
55	Froude number	Payne and Prince modified Froude number criterion	200	128.5	198.05	251.01

Using the equivalent liquid only velocities and flow rates, Wallis (1969) criterion for critical velocity discerns the gas flow regimes of all test groups in stratified basins filled with saltwater of salinity of 25 ppt and 35 ppt at bottom layer. However, in stratified basins filled with saltwater of salinity of 45 ppt and 55 ppt at bottom layer, although the criterion discerns the flow regimes of 1bar and 3bar test group experiments, it does not distinguish the change of flow regime from 1bar to 2bar test group.

Modified Weber number in Zhao and Iron (1990) as well as Tang and Masutani (2003) criterions, determine all test groups in fully developed jetting regime. The modified Weber number in these criterions are of order of 10^3 which is well above the expected limits to distinguish the change of flow regime from 1bar test group to 2bar test group (ranging between 238.78 and 324 for different experiments).

Modified Froude number as introduced by Hoefele and Brimacombe (1979) as well as nominal Mach number criterion (Hoefele & Brimacombe, 1979) predict all test groups in jetting regime. Use of velocity based modified Froude number correlation results in figures of order of 10^4 against the expected limit of ~185 (non-dimensional) to distinguish the change of flow regime. However the modified Froude number correlation based on flow rate, results in figures of order of 10^2. The range of resulted modified Froude numbers from the correlations based on jet flow rate are more acceptable than the velocity based modified Froude number.

Payne and Prince (2003) criterion of modified Froude number results in close discerning of gas flow regimes in all test groups with the basin bottom layers of 25 ppt, 35 ppt and 45 ppt. However, with the basin bottom layer of 55 ppt, although it discerns the flow regimes of 1bar and 3bar test groups experiments, it could not distinguish the change of flow regime from 1bar to 2bar test groups.

The above results were obtained by using the equivalent liquid only flow as the dispersed phase characteristics in the subjected correlations. In Table 3 the correlations output by using the equivalent gas only flow rates and velocities are listed. To obtain the equivalent gas only flow rates and velocities, the momentum exerted by liquid part of the flow is replaced with the equivalent momentum of gas if the only flowing fluid in jet was the gas phase. The following correlation (Eqs. 17 and 18) are derived from the principle of conservation of momentum flux. In the following, M_g and M_l are the exit momentum flux of gas phase and liquid phase in the bubbly water jet respectively and $M_{E,GO}$ is the momentum flux of an equivalent gas only jet. The equivalent gas only velocity is then defined as the velocity of a pure gas jet producing the same momentum flux as the bubbly water jet:

$$M_{E,GO} = M_l + M_g = \rho_l(1-n)AU^2 + \rho_g nAU^2 \tag{17}$$

$$U_{E,GO} = U\left(n + (1-n)\frac{\rho_l}{\rho_g}\right)^{\frac{1}{2}} \tag{18}$$

Here $U_{E,GO}$ is the equivalent gas only flow velocity and A is the nozzle cross section area. Using Eqs. 17 and 18 the equivalent gas only velocity of 1bar, 2bar and 3bar test groups are 93.642 (m/s), 132.116 (m/s) and 155.500 (m/s) respectively and the equivalent gas only flow rates for test groups are 0.000901 (m^3/s), 0.001271 (m^3/s) and 0.001496 (m^3/s) respectively.

Table 3. Gas flow regime criterions in experimental results using equivalent gas only velocities and flow rates.

salinity ppt	Characteristic	Criterion	lower limit for Jetting regime	1bar test group	2bar test group	3bar test group
25	Critical Velocity	Wallis Critical Velocity criterion	7.063	93.642	132.116	155.5
25	Mach number	Hoefele and Brimacombe nominal Mach number criterion	0.2040	0.2730	0.3851	0.4533
25	Weber number	Zhao and Iron critical Weber number criterion	238.02	844.0162	1680.0269	2327.376

25	Weber number	Tang and Masutani modified Weber number criterion	324	844.0162	1680.0269	2327.376
25	Modified Froude number	Hoefele and Brimacombe velocity based modified Froude number criterion	185	497.954	991.186	1373.110
25	Modified Froude number	Hoefele and Brimacombe flow rate based modified Froude number criterion	185	307.163	611.413	847.003
25	Modified Froude number	Payne and Prince modified Froude number criterion	200	22.314	31.4831	37.055
35	Critical Velocity	Wallis Critical Velocity criterion	7.159	93.642	132.116	155.5
35	Mach number	Hoefele and Brimacombe nominal Mach number criterion	0.2046	0.2730	0.3851	0.4533
35	Weber number	Zhao and Iron critical Weber number criterion	238.78	827.050	1646.255	2280.592
35	Weber number	Tang and Masutani modified Weber number criterion	324	827.050	1646.255	2280.592
35	Modified Froude number	Hoefele and Brimacombe velocity based modified Froude number criterion	185	494.787	984.882	1364.377
35	Modified Froude number	Hoefele and Brimacombe flow rate based modified Froude number criterion	185	305.209	607.524	841.616
35	Modified Froude number	Payne and Prince modified Froude number criterion	200	22.243	31.382	36.937
45	Critical Velocity	Wallis Critical Velocity criterion	7.376	93.642	132.116	155.5
45	Mach number	Hoefele and Brimacombe nominal Mach number criterion	0.2054	0.2730	0.3851	0.4533
45	Weber number	Zhao and Iron critical Weber number criterion	239.71	792.617	1577.716	2185.643
45	Weber number	Tang and Masutani modified Weber number criterion	324	792.617	1577.716	2185.643
45	Modified Froude number	Hoefele and Brimacombe velocity based modified Froude number criterion	185	490.944	977.232	1353.780
45	Modified Froude number	Hoefele and Brimacombe flow rate based modified Froude number criterion	185	302.839	602.806	835.080
45	Modified Froude number	Payne and Prince modified Froude number criterion	200	22.157	31.260	36.793
55	Critical Velocity	Wallis Critical Velocity criterion	7.458	93.642	132.116	155.5
55	Mach number	Hoefele and Brimacombe nominal Mach number criterion	0.2062	0.2730	0.3851	0.4533
55	Weber number	Zhao and Iron critical Weber number criterion	240.64	779.091	1550.794	2148.347

55	Weber number	Tang and Masutani modified Weber number criterion	324	779.091	1550.794	2148.347
55	Froude number	Hoefele and Brimacombe velocity based modified Froude number criterion	185	487.160	969.701	1343.347
55	Froude number	Hoefele and Brimacombe flow rate based modified Froude number criterion	185	300.505	598.160	828.644
55	Froude number	Payne and Prince modified Froude number criterion	200	22.071	31.140	36.651

Table 3 shows that the critical velocity criterion of Wallis (1969) predicts all the present experiments in fully developed jetting regime and Payne and Prince (1975) modified Froude number criterion with noticeable underestimation predicts all the experiments in bubbling regime. The results suggest that, using the equivalent gas only flow velocity is not applicable to Wallis critical velocity and Payne and Prince modified Froude number criterions, while by using the equivalent liquid only flow velocity, these two criterions showed to be suitable for discerning the flow regimes of present experiments

Hoefele and Brimacombe nominal Mach number criterion, velocity based modified Froude number criterion and flow rate based modified Froude number criterion as well as Zhao and Iron critical Weber number criterion and Tang and Masutani modified Weber number criterion, predict the flow regime of present research experiments in fully developed jetting regime. The resulted from these correlations when using the equivalent gas only velocities seem to be closer to the lowe limits expected from the criterions when compared with using the equivalent liquid only velocities in the correlations. Although these criterions also fail to predict the flow regimes in present experiments but contrary to Wallis critical velocity criterion and Payne and Prince modified Froude number criterion, the results of these correlations are in justifiable ranges.

4- DISCUSSION

Flow visualization of the experiments showed that the gas flow regime in 1bar test group was in transition from bubbling regime to jetting regime, containing both large bubbles and minute bubbles while in 2bar and 3bar test groups, the flow was in form of jetting (atomization) regime.

The formation process of gas bubbles is affected by surface tension, viscosity, inertia and buoyancy forces while the mechanism of bubble breakup and atomization are based on the concept that the destructive forces due to inertia and turbulence prevail over the resistance forces due to surface tension and viscosity (L. Zhao et al., 2014). Martinez-Bazan et al. (1999) suggest that for the case of submerged bubbles in turbulence water flow, the Ohnesorge number which is the ratio of viscose forces to surface tension forces is very small $(Oh < 10^{-2})$ and internal viscose deformation forces are negligible compared to surface tension forces.

Some researchers suggest that the Reynolds number $(Re > 11000)$ which is the ratio of inertial forces to viscous forces is preferred to identify bubbling-jetting regime (Cai et al., 2010). Also Neto et al. (2008) propose that a minimum value of Re = 8000 is necessary to produce bubbles of approximately uniform sizes, independent from gas to liquid volume fraction in bubbly jets. Presence of irregular bubble sizes consisting of both larger bubbles (with diameters of order of $10^{-3}\ m$) and minute bubbles (with diameters of order of $10^{-4} m$ or less) in 1bar test group experiments $(Re = 15600)$ suggests that Reynolds number is not an unconditional criterion for discerning the transition from bubbling to jetting regime.

Table 2 suggests that by using the equivalent liquid only velocity, Wallis (1969) critical velocity and Payne and Prince (2003) velocity based modified Froude number criterions are more suitable to predict the gas flow regime for the case of gas-saturated liquid blowouts. These two criterions distinguish the change of flow regime from 1bar test group to 2bar test group in experiments with lower bottom layer density ($1017\ kg/m^3$ and $1024\ kg/m^3$), better than the other experiments with higher density at basin bottom layer (1032 kg/m^3 and 1040 kg/m^3). This is consistent with the observations of Mirsandi et al. (2019) which showed that when the liquid density is increased the buoyancy force, which aids the bubble detachment increases therefore the bubble volume and bubble detachment time decrease in favor of leaning the flow regime towards bubbling form.

Experimental results show that the modified Weber number criterion and the majority of modified Froude number criterions, which are based on inertia forces, predict 1bar test group of present research in fully developed jetting (atomizing) regime. Failure of these criterions to discern the change of flow regime from 1bar test group to 2bar test group, suggests that the overestimation of destructive forces might be a reason of this discrepancy when compared with bubbly jets produced by combining liquid pumping with gas pumping.

The lesser than expected destructive forces in gas-saturated liquid blowouts can be explained by sudden separation of gas from the liquid phase at zone of flow establishment, which happens due to sudden pressure drop at nozzle tip. Sudden gas separation from the gas-saturated liquid, forms part of the minute bubbles observed in the plume and reduces the buoyancy of the continues-phase control volume, which consequently reduces the inertia forces. It seems that off-source buoyancy enhancement caused by bubble formation in zone of flow establishment ($z < 0.1l_M$) hampers flow instabilities (Bhat and Narasimha, 1996 and Narasimha et al. 2002). Formation of tiny bubbles will continue further to zone of bubbly jet ($z > 0.1l_M$) and bubbly plume zone ($z > 5l_M$) and disrupts the turbulence and coherent eddy structures in these zones as well, whereas the role of the disrupted turbulences was to provide the lacking amount of energy to obtain the breakup of pre-deformed bubbles (Lima Neto, 2012).

Furthermore, Brandvik et al (2019) reported unexpectedly higher interfacial tensions measured from their live-oil samples that were treated with dispersants. They suggest that the unexpected high interfacial tensions were caused by emulsification due to gas expansion and surfactant interaction with the live oil during depressurization during sampling (Brandvik et al., 2015). The effect of emulsification due to sudden depressurizing and formation of a huge number of tiny bubbles in the zone of flow establishment on the resisting forces (e.g. viscosity and surface tension) requires further investigation. It is worth to note that surface-active agents are usually present in all waters even in laboratory, unless extreme care has been taken specifically to exclude them (Motarjemi & Jameson, 1978).

5- CONCLUSION

More than thirty experimental gas-saturated liquid blowouts tests were visually studied with imaging technique. The most accepted gas flow regime criterions found in literature were employed to predict the gas flow regimes of the experiments. Non-dimensional forms of the criterions for continues-phase flow specifications were defined, using both equivalent liquid only velocities and equivalent gas only velocities.

The results obtained from the criterions suggest that Wallis (1969) and Payne and Prince (1979) criterions are more suitable for discerning the gas flow regimes in gas-saturated liquid blowouts when the equivalent liquid only flow characteristics are applied.

The majority of studied criterions overestimate the ratio of bubble destructive forces (e.g., inertia force) to breakup resisting force (e.g., surface tension and viscosity) in gas-saturated liquid blowouts. The lesser destructive forces in gas-saturated liquid blowouts, when compared to the bubbly jets produced by combining gas pumping with liquid pumping, seem to be due to the effect of off-source bubble formation in the zone of flow establishment. Formation of a huge number concentration of tiny bubbles in the zone of flow establishment and bubbly jet zone causes off-source bouncy enhancement. Off-source buoyancy enhancement disrupts the instabilities, which are the destructive forces in the criterions. Furthermore, the off-source bubble formation process is continued in the bubbly jet zone (momentum-dominated region) and the bubbly plume zone (buoyancy-dominated region), which hampers the turbulence and coherent eddy structures that are the source of providing the lacking energy to obtain the breakup of pre-deformed bubbles.

A reliable estimation of gas flow regimes in live oil blowouts contributes in determining the plume dynamic behavior of pollutants in stratified seawater and can support reasonable pollutant fate prediction and risk evaluation in offshore oil and gas leakage accidents. The results of this work can be useful for users of numerical models in real-world underwater oil and gas blowout fate prediction.

References

[1] Bafandeh, B., Bidokhti, A., Lari, K., & Ezam, M. (2022). Experimental and numerical study of gas to liquid ratio in stratified gas-saturated liquid blowouts' plumes. *International Journal of Environmental Science and Technology, 19*(4), 2365-2378. doi:https://doi.org/10.1007/s13762-021-03343-w

[2] Bie, H.-Y., Ye, J.-J., & Hao, Z.-R. (2016). Effect of nozzle geometry on characteristics of submerged gas jet and bubble noise. *Journal of laboratory automation, 21*(5), 652-659. doi:https://doi.org/10.1177/2211068215584902

[3] Brandvik, P. J., Johansen, Ø., Farooq, U., Davies, E., Krause, D., & Leirvik, F. (2015). Subsurface oil releases–Experimental study of droplet size distributions Phase-II. *Environmental Technology, 2015*, 04-04.

[4] Cai, Q., Shen, X., Shen, C., & Dai, G. (2010). A simple method for identifying bubbling/jetting regimes transition from large submerged orifices using electrical capacitance tomography (ECT). *The Canadian Journal of Chemical Engineering, 88*(3), 340-349. doi:https://doi.org/10.1002/cjce.20295

[5] Clift, R., Grace, J. R., & Weber, M. E. (2005). Bubbles, drops, and particles.

[6] Delnoij, E., Kuipers, J., & van Swaaij, W. P. M. (1997). Dynamic simulation of gas-liquid two-phase flow: effect of column aspect ratio on the flow structure. *Chemical engineering science, 52*(21-22), 3759-3772. doi:https://doi.org/10.1016/S0009-2509(97)00222-4

[7] Goda, T., Iguchi, M., Sasaki, Y., & Kiuchi, H. (2005). Empirical equations for bubble formation frequency from downward-facing nozzle with and without rotating flow effects. *Materials transactions, 46*(11), 2461-2466. doi:https://doi.org/10.2320/matertrans.46.2461

[8] Gros, J., Reddy, C. M., Nelson, R. K., Socolofsky, S. A., & Arey, J. S. (2016). Simulating gas–liquid− water partitioning and fluid properties of petroleum under pressure: implications for deep-sea blowouts. *Environmental science & technology, 50*(14), 7397-7408. doi:https://doi.org/10.1021/acs.est.5b04617

[9] Hoefele, E., & Brimacombe, J. (1979). Flow regimes in submerged gas injection. *Metallurgical Transactions B, 10*(4), 631-648.

[10] Irrgang, C., Hinrichsen, O., & Lau, R. (2012). Effects of orifice angle and surface roughness on the bubbling-to-jetting regime transition in a bubble column. *Industrial & engineering chemistry research, 51*(11), 4445-4451. doi:https://doi.org/10.1021/ie202890u

[11] Johansen, Ø., Brandvik, P. J., & Farooq, U. (2013). Droplet breakup in subsea oil releases–Part 2: Predictions of droplet size distributions with and without injection of chemical dispersants. *Marine Pollution Bulletin, 73*(1), 327-335. doi:https://doi.org/10.1016/j.marpolbul.2013.04.012

[12] Krishnapisharody, K., & Irons, G. (2013). A critical review of the modified Froude number in ladle metallurgy. *Metallurgical and Materials Transactions B, 44*(6), 1486-1498. doi:https://doi.org/10.1007/s11663-013-9943-4

[13] Kubasch, J. H. (2001). *Bubble hydrodynamics in large pools.* ETH Zurich,

[14] Lima Neto, I. E. (2012). Modeling the liquid volume flux in bubbly jets using a simple integral approach. *Journal of hydraulic engineering, 138*(2), 210-215. doi:https://doi.org/10.1061/(ASCE)HY.1943-7900.0000499

[15] Miao, T., Liu, J., Qin, S., Chu, N., Wu, D., & Wang, L. (2018). The flow and acoustic characteristics of underwater gas jets from large vertical exhaust nozzles. *Journal of Low Frequency Noise, Vibration and Active Control, 37*(1), 74-89. doi:https://doi.org/10.1177/1461348418761688

[16] Motarjemi, M., & Jameson, G. (1978). Mass transfer from very small bubbles—the optimum bubble size for aeration. *Chemical engineering science, 33*(11), 1415-1423.

[17] Oguz, H. N., & Prosperetti, A. (1993). Dynamics of bubble growth and detachment from a needle. *Journal of Fluid Mechanics, 257*, 111-145. doi:https://doi.org/10.1017/S0022112093003015

[18] Socolofsky, S. A., & Adams, E. E. (2005). Role of slip velocity in the behavior of stratified multiphase plumes. *Journal of hydraulic engineering, 131*(4), 273-282. doi:https://doi.org/10.1061/(ASCE)0733-9429(2005)131:4(273)

[19] Socolofsky, S. A., Adams, E. E., & Sherwood, C. R. (2011). Formation dynamics of subsurface hydrocarbon intrusions following the Deepwater Horizon blowout. *Geophysical Research Letters, 38*(9). doi:https://doi.org/10.1029/2011GL047174

[20] Sun, Y., Cao, X., Liang, F., & Bian, J. (2020). Investigation on underwater gas leakage and dispersion behaviors based on coupled Eulerian-Lagrangian CFD model. *Process safety and environmental protection, 136*, 268-279. doi:https://doi.org/10.1016/j.psep.2020.01.034

[21] Tsuge, H., Tezuka, Y., & Mitsudani, M. (2006). Bubble formation mechanism from downward nozzle—Effect of nozzle shape and operating parameters. *Chemical engineering science, 61*(10), 3290-3298. doi:https://doi.org/10.1016/j.ces.2005.12.002

[22] Zhao, L., Boufadel, M. C., King, T., Robinson, B., Gao, F., Socolofsky, S. A., & Lee, K. (2017). Droplet and bubble formation of combined oil and gas releases in subsea blowouts. *Marine Pollution Bulletin, 120*(1-2), 203-216. doi:https://doi.org/10.1016/j.marpolbul.2017.05.010

[23] Zhao, L., Boufadel, M. C., Socolofsky, S. A., Adams, E., King, T., & Lee, K. (2014). Evolution of droplets in subsea oil and gas blowouts: Development and validation of the numerical model VDROP-J. *Marine Pollution Bulletin, 83*(1), 58-69. doi:https://doi.org/10.1016/j.marpolbul.2014.04.020

[24] Zhao, Y.-F., & Irons, G. A. (1990). The breakup of bubbles into jets during submerged gas injection. *Metallurgical Transactions B, 21*(6), 997-1003. doi:https://doi.org/10.1007/BF02670270